Physics Letters B 743 (2015) 444–450

Contents lists available at ScienceDirect

Physics Letters B

www.elsevier.com/locate/physletb

Constraints on hard spectator scattering and annihilation corrections in $B_{u,d} \to PV$ decays within QCD factorization

Junfeng Sun [a], Qin Chang [a,b,*], Xiaohui Hu [a], Yueling Yang [a]

[a] Institute of Particle and Nuclear Physics, Henan Normal University, Xinxiang 453007, China
[b] State Key Laboratory of Theoretical Physics, Institute of Theoretical Physics, Chinese Academy of Sciences, China

ARTICLE INFO

Article history:
Received 8 December 2014
Received in revised form 27 February 2015
Accepted 4 March 2015
Available online 6 March 2015
Editor: B. Grinstein

ABSTRACT

In this paper, we investigate the contributions of hard spectator scattering and annihilation in $B \to PV$ decays within the QCD factorization framework. With available experimental data on $B \to \pi K^*, \rho K$, $\pi\rho$ and $K\phi$ decays, comprehensive χ^2 analyses of the parameters $X_{A,H}^{i,f}(\rho_{A,H}^{i,f}, \phi_{A,H}^{i,f})$ are performed, where $X_A^f(X_A^i)$ and X_H are used to parameterize the endpoint divergences of the (non)factorizable annihilation and hard spectator scattering amplitudes, respectively. Based on χ^2 analyses, it is observed that (1) The topology-dependent parameterization scheme is feasible for $B \to PV$ decays; (2) At the current accuracy of experimental measurements and theoretical evaluations, $X_H = X_A^i$ is allowed by $B \to PV$ decays, but $X_H \neq X_A^f$ at 68% C.L.; (3) With the simplification $X_H = X_A^i$, parameters X_A^f and X_A^i should be treated individually. The above-described findings are very similar to those obtained from $B \to PP$ decays. Numerically, for $B \to PV$ decays, we obtain $(\rho_{A,H}^i, \phi_{A,H}^i[^\circ]) = (2.87^{+0.66}_{-1.95}, -145^{+14}_{-21})$ and $(\rho_A^f, \phi_A^f[^\circ]) = (0.91^{+0.12}_{-0.13}, -37^{+10}_{-9})$ at 68% C.L. With the best-fit values, most of the theoretical results are in good agreement with the experimental data within errors. However, significant corrections to the color-suppressed tree amplitude α_2 related to a large ρ_H result in the wrong sign for $A_{CP}^{dir}(B^- \to \pi^0 K^{*-})$ compared with the most recent BABAR data, which presents a new obstacle in solving "$\pi\pi$" and "πK" puzzles through α_2. A crosscheck with measurements at Belle (or Belle II) and LHCb, which offer higher precision, is urgently expected to confirm or refute such possible mismatch.

Nonleptonic decays of hadrons containing a heavy quark play an important role in testing the Standard Model (SM) picture of the *CP* violation mechanism in flavor physics, improving our understanding of nonperturbative and perturbative QCD and exploring new physics beyond the SM. For charmless B meson decays, experimental studies have been successfully carried out at B factories (BABAR and Belle) and Tevatron (CDF and D0) in the past and will be continued by running LHCb and upgrading Belle II experiments. These experiments provide highly fertile ground for theoretical studies and have yielded many exciting and important results, such as measurements of pure annihilation $B_s \to \pi^+\pi^-$ and $B_d \to K^+K^-$ decays reported recently by CDF, LHCb and Belle [1–3], which may suggest the existence of unexpected large annihilation contributions and have attracted much attention, for instance, Refs. [4–10].

Theoretically, to calculate the hadronic matrix elements of hadronic B weak decays, some approaches, including QCD factorization (QCDF) [11], perturbative QCD (pQCD) [12] and soft-collinear effective theory (SCET) [13], have been fully developed and extensively employed in recent years. Even though the annihilation contributions are formally power suppressed in the heavy quark limit, they may be numerically important for realistic hadronic B decays, particularly for pure annihilation processes and direct *CP* asymmetries. Unfortunately, in the collinear factorization approximation, the calculation of annihilation corrections always suffers from end-point divergence. In the pQCD approach, such divergence is regulated by introducing the parton transverse momentum k_T and the Sudakov factor at the expense of modeling the additional k_T dependence of meson wave functions, and large complex annihilation corrections are presented [14]. In the SCET approach, such divergence is removed by separating the physics at different momentum scales and using zero-bin subtraction to avoid double counting the soft degrees of freedom [15,16]; thus, the annihilation diagrams are factorable but real to the leading

* Corresponding author.
E-mail address: changqin@htu.edu.cn (Q. Chang).

http://dx.doi.org/10.1016/j.physletb.2015.03.001

power term of $\mathcal{O}(\alpha_s(m_b)\Lambda_{QCD}/m_b)$. The absence of strong phases from SCET's annihilation amplitudes differs with the pQCD's estimation and the QCDF expectation [17].

Within the QCDF framework, to estimate the annihilation amplitudes and regulate the endpoint divergency, the logarithmically divergent integral is usually parameterized in a model-independent manner [17] and explicitly expressed as

$$\int_0^1 \frac{dx}{x} \to X_A = (1+\rho_A e^{i\phi_A})\ln\frac{m_b}{\Lambda_h}, \tag{1}$$

with the typical scale $\Lambda_h = 0.5$ GeV. Moreover, a similar endpoint singularity also appears in the hard spectator scattering (HSS) contributions of higher twist distribution amplitudes that are also formally power suppressed but chirally enhanced; therefore, a similar parameterization ansatz is used to cope with HSS endpoint divergency, and quantity $X_H(\rho_H, \phi_H)$, similar to the definition of Eq. (1), is introduced. As discussed in Ref. [17], $X_{H,A} \sim \ln(m_b/\Lambda_h)$ is expected because the effects of the intrinsic transverse momentum and off-shellness of partons would be to modify $x \to x+\epsilon$ with $\epsilon \sim \mathcal{O}(\Lambda_{\rm QCD}/m_b)$ in the denominator of Eq. (1). The factor $(1+\rho e^{i\phi})$ summarizes the remaining unknown nonperturbative contributions, where ϕ, which is related to the strong phase, is important for direct CP asymmetries. In such a parameterization scheme, even though the predictive power of QCDF is partly weakened due to the incalculable parameters ρ and ϕ that are introduced, it also provides a feasible way to evaluate the effects and the behavior of annihilation and HSS corrections from a phenomenological view point, which is helpful for understanding and exploring possible underlying mechanisms.

Although the magnitude of and constraints on parameter ρ are utterly unknown based on the first principles of QCD dynamics for now, an excessively large value of ρ would significantly enhance the subleading $1/m_b$ contributions, and hence, a conservative choice of $\rho_A \sim 1$ has typically been used in previous phenomenological studies [17–20]. In practice, different values of (ρ_A, ϕ_A) chosen according to various B meson decay types (PP, PV, VP and VV) have been used to fit experimental data [17,20]. However, with the favored "Scenario S4", in which $\rho_A \simeq 1$ and $\phi_A \simeq -55°$ [17] for $B \to PP$ decay, the QCDF prediction $\mathcal{B}(B_s \to \pi^+\pi^-) = (0.26^{+0.00+0.10}_{-0.00-0.09})\times 10^{-6}$ [20] is about 3.4σ less than the experimental data $(0.73\pm0.14)\times 10^{-6}$ [21].

Motivated by this possible mismatch, detailed analyses have been performed within the QCDF framework [7–10]. In Refs. [7,8], a "new treatment" for endpoint parameters is presented in which the flavor dependence of the annihilation parameter X_A on the initial states should be carefully considered, and hence, X_A is divided into two independent parameters X_A^i and X_A^f, which are responsible for parameterizing the endpoint divergences of nonfactorizable and factorizable annihilation topologies, respectively. Following the proposal of Refs. [7,8] and combining available experimental data for $B_{u,d,s} \to \pi K, \pi\pi$ and $K\bar{K}$ decays, the comprehensive χ^2 analyses of $X_A^{i,f}$ and X_H in $B \to PP$ decays were performed in Refs. [9,22]. It was found that:

- Theoretically, there is neither a compulsory constraint nor a priori reason for both $X_A^i = X_A^f = X_A$ and X_A being universal for all hadronic B decays; Phenomenologically, it is required by available measurements regarding $B \to PP$ decays that X_A^i and X_A^f should be treated individually; in addition, the simplification $X_H = X_A^i$ is allowed by data, which effectively reduces the number of unknown variables, but $X_H \neq X_A^f$ (see scenario III in Ref. [9] for detail);
- The effect of flavor symmetry breaking on parameter $X_A^{i,f}$ is tiny and negligible for the moment due to large experimental errors and theoretical uncertainties;
- A slightly large $\rho_H \sim 3$ with $\phi_H \sim -105°$ and a relatively small inverse moment parameter $\lambda_B \sim 200$ MeV for B meson wave functions are required to enhance the color-suppressed coefficients α_2 with a large strong phase, which is important in accommodating all available observables of $B_{u,d,s} \to \pi K, \pi\pi$ and $K\bar{K}$ decays simultaneously, even the so-called "πK" and "$\pi\pi$" puzzles (see Refs. [9,22] for detail);
- Numerically, in the most simplified scenario in which $X_H = X_A^i$ is assumed, combining the constraints from $B_{u,d,s} \to \pi K, \pi\pi$ and $K\bar{K}$ decays, two solutions responsible for $B \to PP$ decays are obtained [22],

$$\text{Solution A:} \begin{cases} (\rho_{A,H}^i, \phi_{A,H}^i[°]) = (2.98^{+1.12}_{-0.86}, -105^{+34}_{-24}), \\ (\rho_A^f, \phi_A^f[°]) = (1.18^{+0.20}_{-0.23}, -40^{+11}_{-\ 8}), \\ \lambda_B = 0.19^{+0.09}_{-0.04}\ \text{GeV}; \end{cases} \tag{2}$$

$$\text{Solution B:} \begin{cases} (\rho_{A,H}^i, \phi_{A,H}^i[°]) = (2.97^{+1.19}_{-0.90}, -105^{+32}_{-24}), \\ (\rho_A^f, \phi_A^f[°]) = (2.80^{+0.25}_{-0.21}, 165^{+4}_{-3}), \\ \lambda_B = 0.19^{+0.10}_{-0.04}\ \text{GeV}, \end{cases} \tag{3}$$

which yield similar HSS and annihilation contributions.

In recent years, many measurements of $B \to PV$ decays have been performed anew at higher precision [21]. Thus, with the available experimental data, it is worth reexamining the agreement between QCDF's predictions and experimental data on $B \to PV$ decays, investigating the effects of HSS and annihilation contributions, and further testing whether the aforementioned findings regarding $B \to PP$ decays still persist in $B \to PV$ decays. In this paper, we would like to extend our previous studies on $B \to PP$ decays [9,22] to $B \to PV$ decays with the same χ^2 fit method and similar treatment of annihilation and HSS parameters; the details of the statistical χ^2 approach can be found in the appendix of Refs. [9,23].

For $B \to PV$ decays, the decay amplitudes and relevant formulae have been clearly listed in Ref. [17]. The parameters $X_A^{i,f}$ under discussion appear in the basic building blocks of annihilation amplitudes, which can be explicitly written as follows [17]:

$$A_1^i \simeq -A_2^i \simeq 6\pi\alpha_s\Big[3\Big(X_A^i - 4 + \frac{\pi^2}{3}\Big) + r_\chi^{M_1} r_\chi^{M_2}\Big((X_A^i)^2 - 2X_A^i\Big)\Big], \tag{4}$$

$$A_3^i \simeq 6\pi\alpha_s\Big[-3r_\chi^{M_1}\Big((X_A^i)^2 - 2X_A^i - \frac{\pi^2}{3} - 4\Big) + r_\chi^{M_2}\Big((X_A^i)^2 - 2X_A^i - \frac{\pi^2}{3}\Big)\Big], \tag{5}$$

$$A_1^f = A_2^f = 0, \tag{6}$$

$$A_3^f \simeq 6\pi\alpha_s\Big[3r_\chi^{M_1}(2X_A^f - 1)(2 - X_A^f) - r_\chi^{M_2}\Big(2(X_A^f)^2 - X_A^f\Big)\Big], \tag{7}$$

for the VP final state, where the superscript $f(i)$ in $A_k^{f(i)}$ corresponds to (non)factorizable annihilation topologies. For the PV final state, one must simply exchange $r_\chi^{M_1} \leftrightarrow r_\chi^{M_2}$ and change the sign of A_3^f. Further explanation and information on QCDF's annihilation amplitudes can be found in Ref. [17].

Table 1
The *CP*-averaged branching ratios (in units of 10^{-6}) and direct *CP* asymmetries (in units of 10^{-2}) of $B \to \pi K^*, \rho K, \pi\rho$ and KK^* decays. For the theoretical results of Case III, the first and the second theoretical errors are caused by the CKM parameters and the other parameters (including the quark masses, decay constants, form factors and λ_B), respectively.

Decay modes	Branching fractions			Direct *CP* asymmetries		
	Exp.	Case III	S4	Exp.	Case III	S4
$B^- \to \pi^- \bar{K}^{*0}$	10.5 ± 0.8	$8.7^{+0.4+1.3}_{-0.5-1.2}$	8.4	-4.2 ± 4.1	$0.47^{+0.02+0.11}_{-0.02-0.13}$	0.8
$B^- \to \pi^0 K^{*-}$	8.8 ± 1.2	$5.4^{+0.3+0.7}_{-0.3-0.7}$	6.5	-39 ± 12	$0.4^{+0.0+4.0}_{-0.0-4.7}$	-6.5
$\bar{B}^0 \to \pi^+ K^{*-}$	8.4 ± 0.8	$7.5^{+0.4+1.1}_{-0.5-1.0}$	8.1	-23 ± 6	-26^{+1+1}_{-1-1}	-12.1
$\bar{B}^0 \to \pi^0 \bar{K}^{*0}$	3.3 ± 0.6	$2.9^{+0.1+0.5}_{-0.2-0.5}$	2.5	-15 ± 13	-21^{+1+6}_{-1-6}	1.0
$B^- \to \bar{K}^0 \rho^-$	$9.4^{+1.9}_{-3.2}$	$7.9^{+0.4+1.3}_{-0.5-1.1}$	9.7	21^{+31}_{-28}	$1.3^{+0.1+0.1}_{-0.1-0.1}$	0.8
$B^- \to K^- \rho^0$	$3.74^{+0.49}_{-0.45}$	$3.41^{+0.19+0.63}_{-0.21-0.57}$	4.3	37 ± 11	26^{+1+5}_{-1-5}	31.7
$\bar{B}^0 \to K^- \rho^+$	7.0 ± 0.9	$9.0^{+0.5+1.4}_{-0.5-1.3}$	10.1	20 ± 11	27^{+1+3}_{-1-3}	20
$\bar{B}^0 \to \bar{K}^0 \rho^0$	4.7 ± 0.7	$5.5^{+0.3+0.8}_{-0.3-0.7}$	6.2	6 ± 20	15^{+1+3}_{-1-3}	-2.8
$B^- \to \pi^- \rho^0$	$8.3^{+1.2}_{-1.3}$	$6.8^{+0.6+1.2}_{-0.6-1.1}$	12.3	18^{+9}_{-17}	$-6.7^{+0.2+3.2}_{-0.2-3.7}$	-11.0
$B^- \to \pi^0 \rho^-$	$10.9^{+1.4}_{-1.5}$	$10.9^{+0.8+2.7}_{-0.8-2.4}$	10.3	2 ± 11	$8.2^{+0.2+1.6}_{-0.3-1.5}$	9.9
$\bar{B}^0 \to \pi^+ \rho^- + \text{c.c.}$	23.0 ± 2.3	$26.7^{+2.1+5.1}_{-2.2-4.5}$	23.6	–	–	–
$\bar{B}^0 \to \pi^0 \rho^0$	2.0 ± 0.5	$1.2^{+0.1+0.5}_{-0.1-0.5}$	1.1	-27 ± 24	$-3.9^{+0.1+5.0}_{-0.1-5.1}$	10.7
$B^- \to K^- \phi$	8.8 ± 0.5	$9.9^{+0.5+1.6}_{-0.6-1.5}$	11.6	4.1 ± 2.0	$0.72^{+0.02+0.14}_{-0.03-0.16}$	0.7
$\bar{B}^0 \to \bar{K}^0 \phi$	$7.3^{+0.7}_{-0.6}$	$9.3^{+0.4+1.5}_{-0.5-1.4}$	10.5	-1 ± 14	$1.2^{+0.0+0.1}_{-0.0-0.1}$	0.8
$B^- \to K^- K^{*0}$	< 1.1	$0.58^{+0.03+0.09}_{-0.04-0.09}$	0.66	–	$-10.6^{+0.3+3.0}_{-0.4-2.6}$	-9.6
$B^- \to K^{*-} K^0$	–	$0.46^{+0.02+0.08}_{-0.03-0.07}$	0.55	–	$-23.0^{+0.6+2.1}_{-0.8-2.2}$	-21.1
$\bar{B}^0 \to K^+ K^{*-} + \text{c.c.}$	< 0.4	$0.11^{+0.01+0.01}_{-0.01-0.01}$	0.15	–	–	–
$\bar{B}^0 \to K^0 \bar{K}^{*0} + \text{c.c.}$	< 1.9	$0.96^{+0.05+0.13}_{-0.06-0.11}$	1.10	–	–	–

Note: Here we adopt the same definition of direct *CP* asymmetry as HFAG [21].

Before entering further discussion, we would like to note the following: (1) In previous studies, the annihilation parameters were assumed to be process-dependent [17–20] where $(\rho_A^{PV}, \phi_A^{PV})$ and $(\rho_A^{VP}, \phi_A^{VP})$ were introduced to describe nonleptonic B decay into the final states PV and VP decays, respectively; sometimes, additional values of (ρ_A, ϕ_A) for $B \to K\phi$ decays [19] were required. In our analysis, parameters (ρ_A^i, ϕ_A^i) and (ρ_A^f, ϕ_A^f) are topology-dependent. (2) As discussed in Refs. [7–9], parameters $X_A^f(\rho_A^f, \phi_A^f)$ are assumed to be universal for factorizable annihilation amplitudes and free of flavor-symmetry-breaking effects because they are not associated with the wave function of initial B mesons, and the approximations of the asymptotic light cone distribution amplitudes of the final states are used. (3) The wave function of B mesons is involved in the calculation of nonfactorizable annihilation amplitudes. Generally, the momentum fraction of light u, d quarks in $B_{u,d}$ mesons should be different from that of the spectator s quark in B_s meson. The flavor-symmetry-breaking effects might be embodied in parameters $X_A^i(\rho_A^i, \phi_A^i)$. In this paper, only $B_{u,d} \to PV$ decays are considered (most $B_s \to PV$ decays have not been measured), and the isospin symmetry is assumed to be held. (4) Unlike in the case of $B \to PP$ decays, in which both final states are pseudoscalar mesons, the wave functions of the vector mesons are also required to evaluate the hadronic matrix elements of $B \to PV$ decays. Therefore, following the treatment of annihilation parameters presented in Refs. [17–20], the parameters $X_A^{i,f}(\rho_A^{i,f}, \phi_A^{i,f})$ for $B \to PV$ decays are generally different from those for $B \to PP$ decays.

As is well known, for the $b \to s$ transition, the tree contributions are strongly suppressed by the CKM factor $|V_{us}^* V_{ub}| \sim \mathcal{O}(\lambda^4)$, whereas the penguin contributions are proportional to the CKM factor $|V_{cs}^* V_{cb}| \sim \mathcal{O}(\lambda^2)$ [24]. In addition, the nonfactorizable contributions between vertex and HSS corrections largely cancel each other out [17]. Therefore, the weak annihilation amplitudes are important for the $b \to s$ nonleptonic B decays. Large annihilation contributions are derived from the coefficient b_3, because b_3 is proportional to the CKM factor $|V_{cs}^* V_{cb}|$ and sensitive to the annihilation building block A_3^f, which is always accompanied by $N_c C_6$. Hence, it is expected that precise observables of $b \to s$ nonleptonic B decays could introduce stringent restrictions on parameters $X_A^f(\rho_A^f, \phi_A^f)$.

Table 2
The mixing-induced *CP* asymmetries (in units of 10^{-2}). The explanation for the uncertainties is the same as that indicated in Table 1.

Decay modes	Exp.	Case III	S4
$\bar{B}^0 \to \bar{K}^0 \rho^0$	54^{+18}_{-21}	63^{+2+3}_{-2-2}	–
$\bar{B}^0 \to \pi^0 \rho^0$	-23 ± 34	-29^{+5+3}_{-7-5}	–
$\bar{B}^0 \to \bar{K}^0 \phi$	74^{+11}_{-13}	72^{+2+0}_{-2-0}	–

Note: Here we adopt the same definition of mixing-induced *CP* asymmetries as HFAG [21].

For the $b \to d$ transition, the tree contributions are dominant if they exist, whereas the penguin contributions are suppressed due to the cancellation between the CKM factors $V_{ud}^* V_{ub}$ and $V_{cd}^* V_{cb}$ [24]. Large annihilation contributions are derived from the coefficient $b_{1,2}$, which is always accompanied by large Wilson coefficients $C_{1,2}$. For color-suppressed tree-dominated hadronic B decays, the contributions of HSS and factorizable annihilation corrections are particularly important, for example, the resolution of the so-called "$\pi\pi$" puzzle [9]. Therefore, severe restrictions on parameters $X_{A,H}^i$ could be derived from many precise observables of the $b \to d$ nonleptonic B decays.

The decay modes considered in this paper include the penguin-dominated $B \to \pi K^*, \rho K$ decays induced by the $b \to s\bar{q}q$ $(q = u, d)$ transition, the penguin-dominated $B \to \phi K$ decays induced by the $b \to s\bar{s}s$ transition, the tree-dominated $B \to \pi\rho$ decays induced by the $b \to d\bar{q}q$ transition, and the penguin- and annihilation-dominated $B \to KK^*$ decays induced by the $b \to d\bar{s}s$ transition. For the observables of the above-mentioned decay modes, the available experimental data are summarized in the "Exp." columns of Tables 1, 2 and 3, in which most of data are the averaged results

Table 3
The *CP* asymmetry parameters (in units of 10^{-2}). The explanation for the uncertainties is the same as that indicated in Table 1.

CP asymmetry parameters	$\bar{B}^0 \to \pi^+\rho^- + \text{c.c.}$			$\bar{B}^0 \to K^+K^{*-} + \text{c.c.}$			$\bar{B}^0 \to K^0\bar{K}^{*0} + \text{c.c.}$		
	Exp.	Case III	S4	Exp.	Case III	S4	Exp.	Case III	S4
C	-3 ± 6	$4.6^{+0.2+0.8}_{-0.2-0.9}$	5	–	0^{+0+0}_{-0-0}	–	–	$13.0^{+0.5+0.6}_{-0.4-0.7}$	–
S	6 ± 7	$-3.6^{+5.0+1.6}_{-6.8-1.6}$	9	–	12^{+5+0}_{-7-0}	–	–	$4.2^{+0.2+0.7}_{-0.1-0.7}$	–
ΔC	27 ± 6	33^{+1+14}_{-1-15}	0	–	0^{+0+0}_{-0-0}	–	–	$-15.3^{+0.1+9.1}_{-0.1-8.7}$	–
ΔS	1 ± 8	$-1.8^{+0.2+0.9}_{-0.3-0.8}$	-3	–	0^{+0+0}_{-0-0}	–	–	$-25.0^{+0.3+6.4}_{-0.2-5.7}$	–
A_{CP}	-11 ± 3	$-11.8^{+0.4+1.5}_{-0.3-1.7}$	-8	–	0^{+0+0}_{-0-0}	–	–	$-10.7^{+0.3+2.2}_{-0.4-2.1}$	–

Note: Here we adopt the same definition for the parameters $C_{f\bar{f}}$, $S_{f\bar{f}}$, $\Delta C_{f\bar{f}}$, $\Delta S_{f\bar{f}}$ and $A_{CP}^{f\bar{f}}$ as HFAG [21] and choose the final states $f = \rho^+\pi^-$, $K^{*+}K^-$ and $K^{*0}\bar{K}^0$.

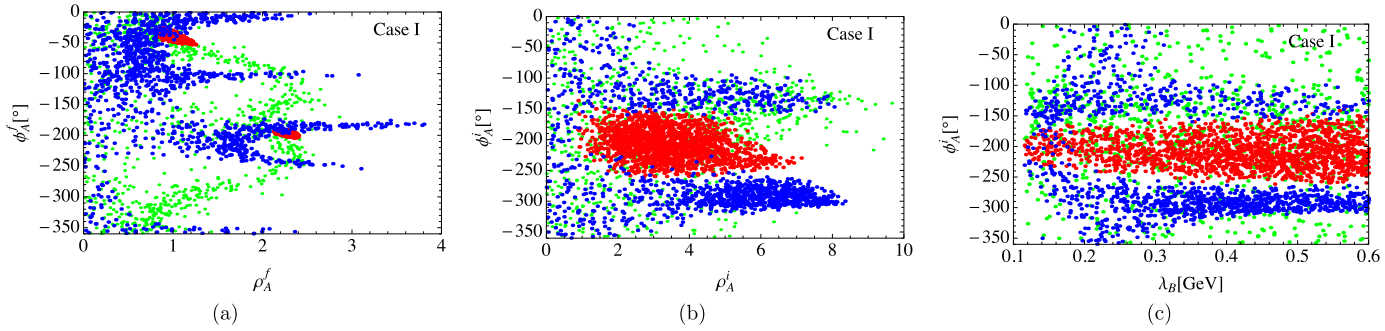

Fig. 1. The allowed regions of parameters $(\rho_A^{i,f}, \phi_A^{i,f})$ and λ_B at 68% C.L. with the constraints from $B \to \pi K^*, \rho K$ decays (red), $B \to \pi\rho$ decays (blue), and $B \to \phi K$ decays (green), respectively. (For interpretation of the references to color in this figure, the reader is referred to the web version of this article.)

given by HFAG [21], except for the branching fractions and direct CP asymmetries of $B^- \to \pi^-\bar{K}^{*0}, \pi^0K^{*-}$ and $\bar{K}^0\rho^-$ decays. Recently, using the full dataset of 470.9 ± 2.8 million $B\bar{B}$ events, the BABAR Collaboration reported the latest results from an analysis of $B^+ \to K^0\pi^+\pi^0$ (and the combined results from this and previous BABAR analyses) [25]

$$B^- \to \pi^-\bar{K}^{*0}: \begin{cases} \mathcal{B}[\times 10^{-6}] = 14.6 \pm 2.4 \pm 1.4^{+0.3}_{-0.4} \\ \quad (11.6 \pm 0.5 \pm 1.1), \\ A_{CP}^{dir}[\%] = -12 \pm 21 \pm 8^{+0}_{-11} \\ \quad (2.5 \pm 5.0 \pm 1.6); \end{cases} \tag{8}$$

$$B^- \to \pi^0K^{*-}: \begin{cases} \mathcal{B}[\times 10^{-6}] = 9.2 \pm 1.3 \pm 0.6^{+0.3}_{-0.5} \\ \quad (8.8 \pm 1.1 \pm 0.6), \\ A_{CP}^{dir}[\%] = -52 \pm 14 \pm 4^{+4}_{-2} \\ \quad (-39 \pm 12 \pm 3); \end{cases} \tag{9}$$

$$B^- \to \bar{K}^0\rho^-: \begin{cases} \mathcal{B}[\times 10^{-6}] = 9.4 \pm 1.6 \pm 1.1^{+0.0}_{-2.6}, \\ A_{CP}^{dir}[\%] = 21 \pm 19 \pm 7^{+23}_{-19}, \end{cases} \tag{10}$$

in which, in particular, the first evidence of a CP asymmetry of $B^- \to \pi^0K^{*-}$ is observed at the 3.4σ significance level. In our following analysis, such (combined) results for $B^- \to \pi^0K^{*-}$ and $\bar{K}^0\rho^-$ decays in Eqs. (9) and (10) are used. For $B^- \to \pi^-\bar{K}^{*0}$ decay, its branching fractions and direct CP asymmetry are also measured by Belle Collaboration [26]; therefore, we adopt the weighted averages of observables, which are presented in Table 1.

The data listed in Tables 1, 2 and 3 demonstrate that the first three sets of decay modes are well measured; therefore, experimental data of these decay modes are used in our fitting. In addition, the theoretical inputs are summarized in Appendix A. Our following analyses and fitting are divided into three cases for different purposes.

(1) For Case I, five parameters, $(\rho_A^{i,f}, \phi_A^{i,f})$ and λ_B, are treated as free parameters, and the simplification $X_H = X_A^i$, which is allowed in $B \to PP$ decays [9], is assumed. Moreover, the constraints from $B \to \pi K^*, \rho K$ decays, $B \to \pi\rho$ decays, and $B \to \phi K$ decays are considered separately. The fitted results are shown in Fig. 1.

Fig. 1 (a) clearly shows that parameters (ρ_A^f, ϕ_A^f) are strictly bound into two separate compact regions (red points) around $(0.9, -40°)$ and $(2.2, -200°)$ by the constraints from $B \to \pi K^*$, ρK decays, which is similar to the case for $B \to PP$ decays (see Eq. (2) and Eq. (3)). Moreover, these two regions overlap with the blue and green dotted regions, which implies that the two solutions of (ρ_A^f, ϕ_A^f) are also allowed by $B \to \pi\rho, \phi K$ decays.

As shown in Fig. 1 (b), under the constraints from $B \to \pi\rho$ decays, the parameters (ρ_A^i, ϕ_A^i) are loosely restricted into two wide bands (blue points) around $\phi_A^i \sim -130°$ and $\sim -300°$ because the experimental precision of the observables, especially the direct *CP* asymmetries, on $B \to \pi\rho$ decays is still very rough. Under the constraints from $B \to \pi K^*$ and ρK decays, (ρ_A^i, ϕ_A^i) are restricted around $\phi_A^i \sim -200°$ (red points) and overlap partly with the blue pointed region, which implies that the allowed spaces of (ρ_A^i, ϕ_A^i) would be seriously shrunken under the combined constraints.

From Fig. 1 (c), parameter λ_B cannot be determined exclusively, although an additional phenomenological condition 115 MeV $\leq \lambda_B \leq$ 600 MeV is imposed during our fit based on the studies of Refs. [17,27–31]. In principle, parameter λ_B is only related to the B wave function and independent of any decay modes. Therefore, in our following analyses, the result $\lambda_B = 0.19^{+0.09}_{-0.04}$ GeV fitted from $B \to PP$ decays [22] will be adopted.

(2) For Case II, to determine whether the simplification $X_H = X_A^i$ is valid for $B \to PV$ decays, both (ρ_H, ϕ_H) and $(\rho_A^{i,f}, \phi_A^{i,f})$ are treated as free parameters. Combining all available constraints from $B \to \pi K^*, \rho K, \pi\rho, \phi K$ decays, the allowed parameter spaces at 68% C.L. are shown in Fig. 2.

Fig. 2 clearly shows that (i) Similarly to Case I, two solutions of (ρ_A^f, ϕ_A^f) with very small uncertainties (red points) are obtained, which are denoted "solution A" for $\phi_A^f \sim -40°$ and "solution B" for $\phi_A^f \sim -200°$ for convenience; Meanwhile, the spaces of (ρ_A^i, ϕ_A^i) are still hardly well bounded (blue points) as in Case I; (ii) The allowed spaces of (ρ_A^f, ϕ_A^f) are small and tight, whereas

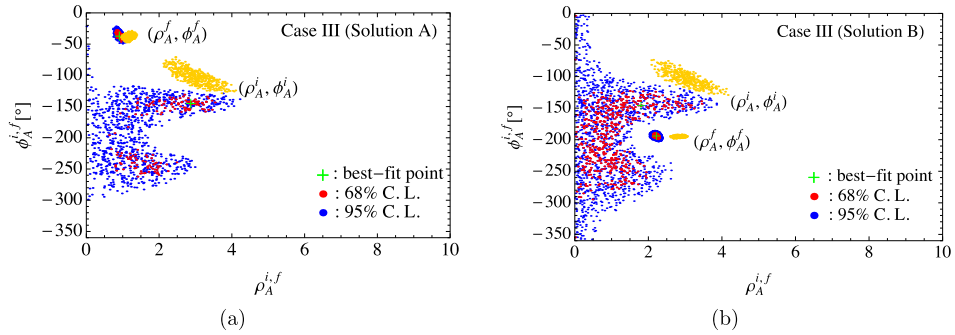

Fig. 3. The allowed regions of parameters $(\rho_A^{i,f}, \phi_A^{i,f})$ at 68% C.L. and 95% C.L. indicated by red and blue points, respectively. The best-fit points of solutions A and B correspond to $\chi^2_{\rm min} = 23$ and 26, respectively. For comparison, the fitted results for $B \to PP$ decays [22] at 68% C.L. are also indicated by yellow points. (For interpretation of the references to color in this figure, the reader is referred to the web version of this article.)

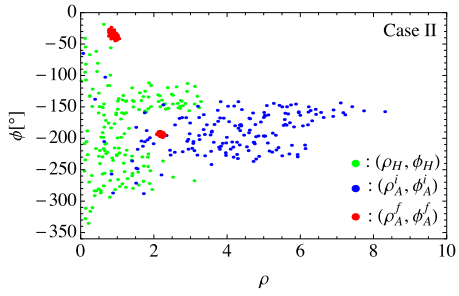

Fig. 2. The allowed regions of parameters $(\rho_{A,H}^{i,f}, \phi_{A,H}^{i,f})$ at 68% C.L. (For interpretation of the references to color in this figure, the reader is referred to the web version of this article.)

those of (ρ_A^i, ϕ_A^i) are big and loose; thus, they generally differ from each other. This finding implies that X_A^f and X_A^i may be treated individually, as in the case for $B \to PP$ decays discussed in Refs. [9,22], which provides further evidence to support the speculation regarding the topology-dependent annihilation parameters reported in Refs. [7,8]; (iii) Interestingly, the spaces of (ρ_H, ϕ_H) (green points) are significantly separated from those of (ρ_A^f, ϕ_A^f) but overlap partly with the regions of (ρ_A^i, ϕ_A^i), which implies that the simplification $X_H \simeq X_A^i$ is roughly allowed for $B \to PV$ decays as in the case of $B \to PP$ decays [22].

(3) For Case III, based on the above-described analysis, we will present the most simplified scenario with four free parameters, i.e., (ρ_A^f, ϕ_A^f) and $(\rho_A^i, \phi_A^i) = (\rho_H, \phi_H)$. Combining the constraints from 35 independent observables of $B \to \pi K^*, \rho K, \pi\rho, \phi K$ decays, our fitted results are shown in Fig. 3, where "solutions A and B" correspond to the minimal values $\chi^2_{\rm min} = 23$ and 26, respectively. Strictly speaking, solution A should be favored over solution B because $\chi^2_{\rm min,A} < \chi^2_{\rm min,B}$. For solution A, the allowed spaces of (ρ_A^i, ϕ_A^i) at 68% C.L. consist of two separate parts located on two sides of $\rho_A^i = -180°$. Corresponding to the best-fit point of solution A, the numerical results of the end-point parameters are

$$(\rho_{A,H}^i, \phi_{A,H}^i[°]) = (2.87^{+0.66}_{-1.95}, -145^{+14}_{-21}),$$
$$(\rho_A^f, \phi_A^f[°]) = (0.91^{+0.12}_{-0.13}, -37^{+10}_{-9}). \quad (11)$$

From Fig. 3, it is observed that (i) Similarly to Case II, the parameters (ρ_A^f, ϕ_A^f) are severely restricted to two small and tight spaces. (ii) In contrast with Case II, the allowed regions of parameters (ρ_A^i, ϕ_A^i) at 68% C.L. shrink notably due to the simplification $X_H = X_A^i$. (iii) The allowed regions of parameters (ρ_A^f, ϕ_A^f) are completely separated from those of (ρ_A^i, ϕ_A^i), which implies that the factorizable annihilation parameters X_A^f should be different from the nonfactorizable annihilation parameters X_A^i. (iv) The spaces of $(\rho_A^{i,f}, \phi_A^{i,f})$ for $B \to PV$ decays are separated from the spaces of $B \to PP$ decays (yellow points in Fig. 3), which implies that parameters X_A for $B \to PP$ and PV decays should be introduced and treated individually.

Using the best-fit (central) values of solution A in Eq. (11), we present the theoretical results for the branching fractions and CP asymmetries of $B \to PV$ decays in the "Case III" columns of Tables 1, 2 and 3. For comparison, the theoretical results of "Scenario S4" [17], with $(\rho_A^{PV}, \rho_A^{PV}) = (1, -20°)$ and $(\rho_A^{VP}, \rho_A^{VP}) = (1, -70°)$, are also listed in the "S4" columns of the tables. It is observed that most of our theoretical results are consistent with the experimental data except for a few contradictions in the $B^- \to \pi^0 K^{*-}$ decay, which will be discussed later, and are similar to the "S4" results.

For the well-measured observables, such as the branching ratios $\mathcal{B}(B \to \phi K)$, $\mathcal{B}(B^- \to \pi^- \rho^0)$, $\mathcal{B}(B^0 \to K\rho)$ with a significance level $\geq 6\sigma$ (see Table 1), the direct CP asymmetry for $\bar{B}^0 \to \pi^+ K^{*-}$ decay (see Table 1) and ΔC for $B \to \pi^\pm \rho^\mp$ decay (see Table 3) with a significance level $\geq 4\sigma$, compared with the traditional "S4" results, our results are more in line with the experimental data. In particular, compared with the measurement $\Delta C = (27 \pm 6)\%$ for $B \to \pi^\pm \rho^\mp$ decay, the difference between the "S4" results and ours is clear and notable, which may imply that a relatively large $\rho_{A,H}^i \sim 3$ rather than the conventionally used small $\rho_A^i \sim 1$ [17–20] may be necessary for nonfactorizable annihilation corrections. In addition, evidence of a large ρ_A for $B \to K\rho, K^*\pi$ decays is also presented in Fig. 3 of Ref. [6] using a similar χ^2 fit approach, with the simplification that $X_A^i = X_A^f$.

Unfortunately, with the central values presented in Eq. (11), from the results gathered in Table 1, one may find that our result $A_{CP}^{dir}(B^- \to \pi^0 K^{*-}) = (0.4^{+0.0+4.0}_{-0.0-4.7})\%$ is significantly larger than the data $(-39 \pm 12)\%$ reported by BABAR. To clarify the reason for this discrepancy, we present the dependence of $A_{CP}^{dir}(B^- \to \pi^0 K^{*-})$ on ϕ_H, ϕ_A^i and ϕ_A^f in Fig. 4. It is easily observed that the best-fit result $(\rho_A^f, \phi_A^f) \sim (0.91, -37°)$ is favored by the BABAR data. However, the best-fit value $(\rho_{A,H}^i, \phi_{A,H}^i) \sim (2.87, -145°)$ results in the large mismatch for $A_{CP}^{dir}(B^- \to \pi^0 K^{*-})$ (in Eq. (11), a small ρ_H is also allowed at 68% C.L., which would yield a better agreement but result in a relative larger χ^2). One interesting and important problem is that a relatively large $\rho_H \sim 3$ in $B \to PP$ decays, which is similar to the best-fit value for $B \to PV$ decays in this work, is always required to enhance α_2 contributions in resolving the "$\pi\pi$" and "πK" puzzles [9,22] but clearly leads to a wrong sign for $A_{CP}^{dir}(B^- \to \pi^0 K^{*-})$ when confronted with BABAR data, as indicated herein and in Ref. [32]. Therefore, if a large negative $A_{CP}^{dir}(B^- \to \pi^0 K^{*-})$ is confirmed by Belle (or future Belle II) and LHCb Collaborations, resolving the "$\pi\pi$" and "πK" puzzles

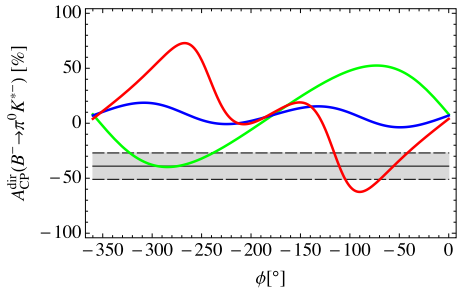

Fig. 4. The green, blue and red lines correspond to the dependence of $A_{CP}^{dir}(B^- \to \pi^0 K^{*-})$ on ϕ_H, ϕ_A^i and ϕ_A^f, with $\rho_H = 3$ ($\rho_A^{i,f} = 0$), $\rho_A^i = 3$ ($\rho_{A,H}^f = 0$) and $\rho_A^f = 1$ ($\rho_{A,H}^i = 0$), respectively. The shaded region corresponds to experimental data (1σ error bar). (For interpretation of the references to color in this figure, the reader is referred to the web version of this article.)

through color-suppressed tree amplitude α_2 will be challenging. If so, a large complex electroweak amplitude $\alpha_{3,EW}$ is probably required [32], which may hint possible new physics effects. In addition, the measurements for observables of $B_s \to \phi\pi^0$ decay, whose amplitude is related to α_2 and $\alpha_{3,EW}$ only, may provide a clue even though such decay mode is not easily to be measured soon.

For the color-suppressed tree-dominated $B \to \pi^0\rho^0$ decay, the penguin-dominated $B^- \to KK^*$ decays and the pure annihilation $\bar{B}^0 \to K^\pm K^{*\mp}$ decay, the decay amplitudes are sensitive to the nonfactorizable HSS and annihilation corrections, and their measurements could perform strong constraints on $X_{A,H}^i(\rho_{A,H}^i, \phi_{A,H}^i)$. Unfortunately, the experimental errors of the observables for $B \to \pi^0\rho^0$ decay are too large, and the $B^- \to KK^*$ and $\bar{B}^0 \to K^\pm K^{*\mp}$ decays have not yet been observed. Future refined measurements conducted at the LHCb and Belle II would be very helpful in carefully examining the HSS and annihilation corrections. Recently, the LHCb Collaboration has updated the upper limit of branching fractions for pure annihilation $\bar{B}^0 \to K^\pm K^{*\mp}$ decay with $< 0.4(0.5)\times 10^{-6}$ at 90 (95%) C.L. [33], and it is eagerly expected that these decays can be precisely measured, which should be useful in probing the annihilation corrections and the corresponding mechanism. Of course, one can use different mechanisms for enhancing the nonfactorizable contributions in QCDF, for example, the final state rescattering effects advocated in Refs. [18–20], in which the allowed regions for parameters $(\rho_{A,H}^i, \phi_{A,H}^i)$ might be different.

In summary, we studied the contributions of HSS and annihilation in $B \to PV$ decays within the QCDF framework. Unlike the traditional treatment of annihilation endpoint divergence with process-dependent parameters $(\rho_A^{PV}, \phi_A^{PV})$ and $(\rho_A^{VP}, \phi_A^{VP})$ in previous studies [17–20], the topology-dependent parameters $(\rho_A^{i,f}, \phi_A^{i,f})$ based on a recent analysis of $B \to PP$ decays [7–9,22] were used in this paper. Combining available experimental data, we performed comprehensive χ^2 analyses of $B \to PV$ decays and obtained information and constraints regarding the parameters $(\rho_A^{i,f}, \phi_A^{i,f})$. It is observed that most of the measurements on observables of $B \to PV$ decays, except for some contradictions in $B^- \to \pi^0 K^{*-}$ decay, could be properly interpreted with the best-fit values presented in Eq. (11), which suggests that the topology-dependent parameterization of annihilation and HSS corrections may be suitable. The other findings of this study are summarized as follows:

- The relatively small value of the B wave function parameter $\lambda_B \sim 0.2$ GeV, which is only related to the universal B wave functions and plays an important role in providing a possible solution to the so-called "$\pi\pi$" and "πK" puzzles [9], is also allowed by the constraints from $B \to PV$ decays.
- As used extensively in phenomenological studies on hadronic B decays [17–20], generally, parameters $X_{A,H}^{i,f}$ for $B \to PP$ and PV decays should be independent of each other and be treated individually.
- The allowed regions of parameters (ρ_A^f, ϕ_A^f) are strictly constrained by available experimental data, whereas the accessible spaces of parameters (ρ_A^i, ϕ_A^i) are relatively large. Generally, there is no common space between (ρ_A^f, ϕ_A^f) and (ρ_A^i, ϕ_A^i) with the approximation of $X_A^i = X_H$, which implies that factorizable annihilation parameters X_A^f should be different from nonfactorizable annihilation parameters X_A^i. Moreover, a relatively large $\rho_A^i \sim 3$ is required by the considerable fine-tuning of $X_A^{i,f}$ to reproduce most of the measurements on hadronic B decays. The above-described evidence and features have been clearly observed in both $B \to PP$ decays [7–9,22] and $B \to PV$ decays.
- Unfortunately, a relatively large $\rho_H \sim 3$ with $\phi_H \sim -145^\circ$ related to significant HSS corrections to color-suppressed tree amplitude α_2, which is helpful for resolving the "$\pi\pi$" and "πK" puzzles and allowed by most $B \to PP$ and PV decays, result in a wrong sign for $A_{CP}^{dir}(B^- \to \pi^0 K^{*-})$ when confronted with recent BABAR data $(-39\pm12)\%$. This finding suggests a large, complex electroweak amplitude attributed to possibly new physics or an undiscovered mechanism [32], which deserves much attention. Before we know for sure, the cross-check based on refined measurements conducted at Belle (Belle II) and LHCb is urgently awaited.

Overall, the annihilation and HSS contributions in nonleptonic B decays should be and have been attracting much attention and careful study. For $B \to PV$ decays, a comparative advantage is that there are more decay modes and more observables than those for $B \to PP$ decays, and hence more information and more stringent constraints on parameters $X_{A,H}$ can be obtained, which represents an opportunity as well as a challenge in the rapid accumulation of data on B events at running LHCb and forthcoming Belle II/SuperKEKB. Theoretically, these results will surely help us to further understand the underlying mechanism of annihilation and HSS contributions and develop more efficient approaches to calculate hadronic matrix elements.

Acknowledgements

This work is supported by the National Natural Science Foundation of China (Grant Nos. 11475055, 11105043, 11147008, 11275057 and U1232101). Q. Chang is also supported by the Foundation for the Author of National Excellent Doctoral Dissertation of the People's Republic of China (Grant No. 201317) and the Program for Science and Technology Innovation Talents in Universities of Henan Province (Grant No. 14HASTIT036). We also thank the Referee and Hai-Yang Cheng for their helpful comments.

Appendix A. Theoretical input parameters

For the CKM matrix elements using the Wolfenstein parameterization, we adopt the fitting results given by the CKMfitter group [34]

$$\bar{\rho} = 0.1453^{+0.0133}_{-0.0073}, \quad \bar{\eta} = 0.343^{+0.011}_{-0.012},$$
$$A = 0.810^{+0.018}_{-0.024}, \quad \lambda = 0.22548^{+0.00068}_{-0.00034}.$$

The pole and running masses of quarks used in our analysis are [24]

$$m_{u,d,s} = 0, \quad m_c = 1.67\pm0.07\ \text{GeV}, \quad m_b = 4.78\pm0.06\ \text{GeV},$$
$$\frac{\bar{m}_s(\mu)}{\bar{m}_q(\mu)} = 27.5\pm1.0, \quad \bar{m}_s(2\ \text{GeV}) = 95\pm5\ \text{MeV},$$
$$\bar{m}_b(\bar{m}_b) = 4.18\pm0.03\ \text{GeV},$$

where $m_q = m_u = m_d = (m_u + m_d)/2$.

The decay constants of pseudoscalar and vector mesons are [24,35,36]

$$f_B = (190.6\pm4.7)\ \text{MeV}, \quad f_\pi = (130.41\pm0.20)\ \text{MeV},$$
$$f_K = (156.2\pm0.7)\ \text{MeV},$$
$$f_\rho = (216\pm3)\ \text{MeV}, \quad f_\rho^\perp(1\ \text{GeV}) = (165\pm9)\ \text{MeV},$$
$$f_{K^*} = (220\pm5)\ \text{MeV}, \quad f_{K^*}^\perp(1\ \text{GeV}) = (185\pm10)\ \text{MeV}.$$

The heavy-to-light transition form factors are [37]

$$F_1^{B\to\pi} = 0.258\pm0.031, \quad F_1^{B\to K} = 0.331\pm0.041,$$
$$A_0^{B\to\rho} = 0.303\pm0.029, \quad A_0^{B\to K^*} = 0.374\pm0.034.$$

The Gegenbauer moments are [38]

$$a_1^\pi = 0, \quad a_2^\pi(1\ \text{GeV}) = 0.25,$$
$$a_1^K(1\ \text{GeV}) = 0.06, \quad a_2^K(1\ \text{GeV}) = 0.25,$$
$$a_{1,\rho}^{\parallel} = 0, \quad a_{2,\rho}^{\parallel}(1\ \text{GeV}) = 0.15,$$
$$a_{1,K^*}^{\parallel}(1\ \text{GeV}) = 0.03, \quad a_{2,K^*}^{\parallel}(1\ \text{GeV}) = 0.11.$$

For other inputs, such as the masses and lifetimes of mesons, we adopt the values given by PDG [24].

References

[1] T. Aaltonen, et al., CDF Collaboration, Phys. Rev. Lett. 108 (2012) 211803.
[2] R. Aaij, et al., LHCb Collaboration, J. High Energy Phys. 1210 (2012) 037.
[3] Y. Duh, et al., Belle Collaboration, Phys. Rev. D 87 (2013) 031103.
[4] Z. Xiao, W. Wang, Y. Fan, Phys. Rev. D 85 (2012) 094003.
[5] M. Gronau, D. London, J. Rosner, Phys. Rev. D 87 (2013) 036008.
[6] C. Bobeth, M. Gorbahn, S. Vickers, arXiv:1409.3252.
[7] G. Zhu, Phys. Lett. B 702 (2011) 408.
[8] K. Wang, G. Zhu, Phys. Rev. D 88 (2013) 014043.
[9] Q. Chang, J. Sun, Y. Yang, X. Li, Phys. Rev. D 90 (2014) 054019.
[10] Q. Chang, X. Cui, L. Han, Y. Yang, Phys. Rev. D 86 (2012) 054016.
[11] M. Beneke, G. Buchalla, M. Neubert, C. Sachrajda, Phys. Rev. Lett. 83 (1999) 1914;
M. Beneke, G. Buchalla, M. Neubert, C. Sachrajda, Nucl. Phys. B 591 (2000) 313.
[12] Y. Keum, H. Li, A. Sanda, Phys. Lett. B 504 (2001) 6;
Y. Keum, H. Li, A. Sanda, Phys. Rev. D 63 (2001) 054008.
[13] C. Bauer, S. Fleming, M. Luke, Phys. Rev. D 63 (2000) 014006;
C. Bauer, S. Fleming, D. Pirjol, I. Stewart, Phys. Rev. D 63 (2001) 114020;
C. Bauer, I. Stewart, Phys. Lett. B 516 (2001) 134;
C. Bauer, D. Pirjol, I. Stewart, Phys. Rev. D 65 (2002) 054022.
[14] C.D. Lu, K. Ukai, M.Z. Yang, Phys. Rev. D 63 (2001) 074009.
[15] A.V. Manohar, I.W. Stewart, Phys. Rev. D 76 (2007) 074002.
[16] C.M. Arnesen, Z. Ligeti, I.Z. Rothstein, I.W. Stewart, Phys. Rev. D 77 (2008) 054006.
[17] M. Beneke, G. Buchalla, M. Neubert, C. Sachrajda, Nucl. Phys. B 606 (2001) 245;
M. Beneke, M. Neubert, Nucl. Phys. B 651 (2003) 225;
M. Beneke, M. Neubert, Nucl. Phys. B 675 (2003) 333.
[18] H. Cheng, C. Chua, Phys. Rev. D 80 (2009) 074031.
[19] H. Cheng, C. Chua, Phys. Rev. D 80 (2009) 114008.
[20] H. Cheng, C. Chua, Phys. Rev. D 80 (2009) 114026.
[21] Y. Amhis, et al., HFAG Collaboration, arXiv:1207.1158; online update at: http://www.slac.stanford.edu/xorg/hfag.
[22] Q. Chang, J. Sun, Y. Yang, X. Li, Phys. Lett. B 740 (2015) 56.
[23] L. Hofer, D. Scherer, L. Vernazza, J. High Energy Phys. 1102 (2011) 080.
[24] K. Olive, et al., Particle Data Group, Chin. Phys. C 38 (2014) 090001.
[25] J.P. Lees, et al., BABAR Collaboration, arXiv:1501.00705.
[26] A. Garmash, et al., Belle Collaboration, Phys. Rev. Lett. 96 (2006) 251803.
[27] G. Bell, V. Pilipp, Phys. Rev. D 80 (2009) 054024.
[28] B. Aubert, et al., BABAR Collaboration, Phys. Rev. D 80 (2009) 111105.
[29] M. Beneke, S. Jäger, Nucl. Phys. B 751 (2006) 160;
M. Beneke, T. Huber, X. Li, Nucl. Phys. B 832 (2010) 109.
[30] M. Beneke, J. Rohrwild, Eur. Phys. J. C 71 (2011) 1818.
[31] V. Braun, A. Khodjamirian, Phys. Lett. B 718 (2014) 1014.
[32] H. Cheng, C. Chiang, A. Kuo, Phys. Rev. D 91 (1) (2015) 014011.
[33] R. Aaij, et al., LHCb Collaboration, arXiv:1407.7704.
[34] J. Charles, et al., CKMfitter Group, Eur. Phys. J. C 41 (2005) 1; online update at: http://ckmfitter.in2p3.fr.
[35] J. Laiho, E. Lunghi, R. Water, Phys. Rev. D 81 (2010) 034503; online update at: http://www.latticeaverages.org.
[36] P. Ball, G. Jones, R. Zwicky, Phys. Rev. D 75 (2007) 054004.
[37] P. Ball, R. Zwicky, Phys. Rev. D 71 (2005) 014015;
P. Ball, R. Zwicky, Phys. Rev. D 71 (2005) 014029.
[38] P. Ball, V. Braun, A. Lenz, J. High Energy Phys. 0605 (2006) 004;
P. Ball, G. Jones, J. High Energy Phys. 0703 (2007) 069.